

The Long Wavelength Array

Now under development, with stations eventually to be distributed over the state of New Mexico, this multipurpose telescope is expected to provide improved angular resolution and sensitivity at frequencies below 88 MHz.

By STEVEN W. ELLINGSON, *Senior Member IEEE*, TRACY E. CLARKE, AARON COHEN, JOSEPH CRAIG, *Member IEEE*, NAMIR E. KASSIM, YLVA PIHLSTRÖM, LEE J RICKARD, AND GREGORY B. TAYLOR

ABSTRACT | The Long Wavelength Array (LWA) will be a new multipurpose radio telescope operating in the frequency range 10–88 MHz. Upon completion, the LWA will consist of 53 phased array “stations” distributed over a region about 400 km in diameter in the state of New Mexico. Each station will consist of 256 pairs of dipole-type antennas whose signals are formed into beams, with outputs transported to a central location for high-resolution aperture synthesis imaging. The resulting image sensitivity is estimated to be a few millijanskys (5σ , 8 MHz, two polarizations, 1 h, zenith) in 20–80 MHz; with resolution and field of view of ($8''$, 8°) and ($2''$, 2°) at 20 and 80 MHz, respectively. Notable engineering features of the instrument, demonstrated in this paper, include Galactic-noise limited active antennas and direct sampling digitization of the entire tuning range. This paper also summarizes the LWA science goals, specifications, and analysis leading to top-level design decisions.

KEYWORDS | Aperture synthesis imaging; digital beamforming; radio astronomy

I. INTRODUCTION

Radio astronomy emerged at frequencies below 100 MHz, a regime from which scientific and technical innovations

flowed that helped lay the basis of modern astronomy for several decades [1]. Important contributions made at these frequencies include the discovery of the importance of nonthermal processes in astrophysics, the discovery of pulsars and Jovian radio emission, progress in understanding space weather, and the development of interferometry and aperture synthesis imaging [2]–[4]. Interest in the field eventually receded because of an inability to compete with the science accessible to large centimeter-wavelength aperture synthesis radio telescopes such as the Very Large Array (VLA) of the National Radio Astronomy Observatory. Specifically, early calibration techniques were incapable of compensating for wavelength-dependent ionospheric phase fluctuations, limiting baselines below 100 MHz to a few kilometers, thereby greatly limiting both resolution and sensitivity.

Several factors have contributed to revive interest in low frequency radio astronomy. In the early 1990s, self-calibration [5] was first successfully applied to overcome the ionospheric limit to short baselines and permit subarc-minute resolution at 74 MHz on the VLA [6], [7]. Over the same time frame, cost and technology for receivers and digital signal processing suitable for large wide-bandwidth beamforming arrays improved dramatically, making it reasonable to consider building low frequency radio telescope arrays whose full resolution, bandwidth, and sensitivity could finally be utilized. Also, advances in computing have made the computationally tedious tasks of radio-frequency interference (RFI) mitigation, calibration, and wide-field image processing tractable. Lastly, an increasing number of questions in astrophysics have emerged in which high-angular-resolution low-frequency radio astronomy plays an important or essential role [4].

The Long Wavelength Array (LWA) is a large multipurpose radio telescope that is being developed to investigate these questions [8].¹ Upon completion, LWA

Manuscript received October 31, 2008; revised January 26, 2009. First published June 23, 2009; current version published July 15, 2009. The LWA is supported by the Office of Naval Research through a contract with the University of New Mexico. Basic research at U.S. Naval Research Laboratory is supported by 6.1 base funds.

S. W. Ellingson is with the Bradley Department of Electrical and Computer Engineering, Virginia Polytechnic Institute and State University, Blacksburg, VA 24061 USA (e-mail: ellingson@vt.edu).

T. E. Clarke, **A. Cohen**, and **N. E. Kassim** are with the U.S. Naval Research Laboratory, Washington, DC 20375 USA (e-mail: tracy.clarke@nrl.navy.mil; Aaron.Cohen@nrl.navy.mil; namir.kassim@nrl.navy.mil).

J. Craig and **L. J. Rickard** are with the LWA Project Office, University of New Mexico, Albuquerque, NM 87131 USA (e-mail: joecraig@unm.edu; lrickard@unm.edu).

Y. Pihlström and **G. B. Taylor** are with the Department of Physics and Astronomy, University of New Mexico, Albuquerque, NM 87131 USA (e-mail: ylva@unm.edu; gbtaylor@unm.edu).

Digital Object Identifier: 10.1109/JPROC.2009.2015683

¹<http://lwa.unm.edu>.



Fig. 1. Artist's concept of an LWA station.

will consist of 53 electronically steered phased array “stations,” each consisting of 256 pairs of dipole-like antennas, operating with Galactic noise-limited sensitivity over the frequency range 10–88 MHz. An LWA station is shown in Fig. 1. The stations will be distributed over the state of New Mexico, as shown in Fig. 2, with maximum baselines (distances between stations) of up to 400 km. Beams formed by the stations will be transmitted to a central location and correlated to form images using aperture synthesis techniques [9]. Stations will also be capable of operating as independent radio telescopes.

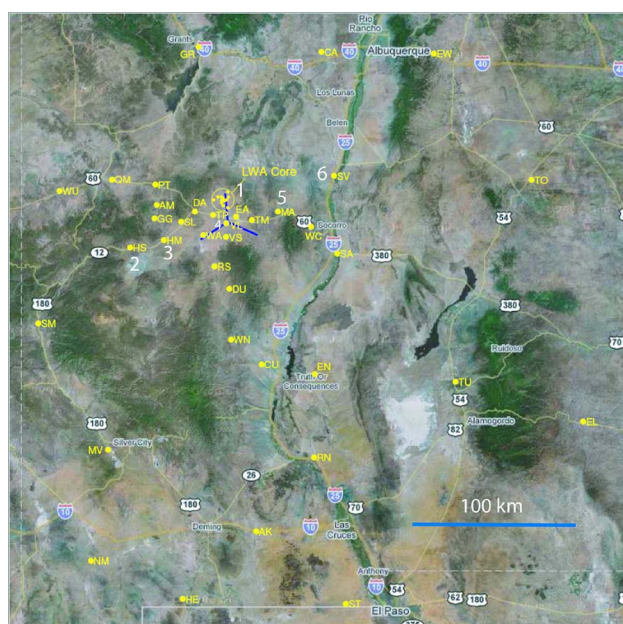


Fig. 2. LWA station locations. Number indicates planned order of installation.

This paper reviews the scientific motivation for LWA and the design as it now exists. The LWA science case and the resulting technical requirements are described in Section II. Sections III and IV address the station- and interferometer-level designs, respectively. In Section V, we compare LWA with the Low Frequency Array (LOFAR) [10],² a similar instrument now under construction in The Netherlands, and discuss plans for construction and operations. Additional detailed information on LWA is available through an online memo series.³

II. SCIENCE CASE AND TECHNICAL REQUIREMENTS

The LWA is designed for both long-wavelength astrophysics and ionospheric science. Science to be addressed by the LWA includes cosmic evolution, the acceleration of relativistic particles, physics of the interstellar and intergalactic media, solar science and space weather, and “discovery science;” that is, the search for previously unknown sources and phenomena [8]. Specific objectives for LWA are spelled out in [11] and are summarized here.

The overarching motivation for LWA is to achieve long-wavelength imaging with angular resolution and sensitivity comparable to existing instruments operating at shorter wavelengths; i.e., on the order of arcseconds and millijanskys (mJy; $1 \text{ Jy} = 10^{-26} \text{ W m}^{-2} \text{ Hz}^{-1}$), respectively. This represents an improvement by two to three orders of magnitude over previous instruments operating at these frequencies. Baselines of up to 400 km yield resolution of 8 and $2''$ at 20 and 80 MHz respectively, required for studying the details of acceleration processes from supernova remnants (SNRs) [12] to the jets [13] and hotspots [14] of extragalactic radio galaxies. Longer baselines bring diminishing returns due to the intrinsic scattering limits imposed by the interplanetary and interstellar media.

LWA is designed to achieve image thermal noise sensitivity on the order of 5 mJy (5σ , 8 MHz, 1 h, zenith) over 20–80 MHz. This approaches the desired millijansky goal while achieving a balance with *confusion*; i.e., the limitation on image sensitivity due to both unresolved sources (“classical confusion”) as well as from bright sources received through sidelobes (“sidelobe confusion”). The angular resolution is sufficient to avoid confusion for plausible integration times (tens to hundreds of hours) over most of the frequency range [15].

While most science will benefit from high sensitivity, specific drivers include the search for extrasolar planets by Jupiter-type decametric radio emission [16], [17] and the detection and study of high redshift radio galaxies [18], [19]. Determination of the total number of antennas (collecting area) and the receiver noise temperature required to achieve this sensitivity is a complex issue, addressed in detail in Section III.

²See <http://www.lofar.org>.

³See <http://www.phys.unm.edu/~lwa/memos>.

Antenna data are aggregated at the station level into beams. The imaging field of view (FOV) is limited by the width of the station beam, which in turn is determined by the dimensions of the station array. A requirement of ~ 100 m mean dimension for the station array balances the desire to efficiently sample large fields and astrophysical sources including SNRs and coronal mass ejections against the increasing difficulty of ionospheric calibration across a wide FOV.

A separate but related issue is the number of stations N_S . It is desirable to concentrate the antennas into a small number of stations so as to simplify the process of acquiring land, transporting data, and maintaining the instrument. At the same time, image quality is determined by the number of baselines as well as their lengths and orientations, which argues for large N_S . Diversity of baselines is particularly important given the wide range of angular scales of interest and the desire for high-dynamic-range imaging in the presence of a complex sky brightness distribution. Guidance for estimating N_S is derived from experience with the VLA. The VLA is a 27-element array that can be arranged in four different configurations, yielding $\sim 2 \times (27)(27 - 1)/2 = 702$ baselines since about half the baselines are shared between configurations. LWA stations cannot be moved, so 53 stations provide roughly twice as many baselines (1378) as the VLA, and should be adequate for imaging the intrinsically larger fields seen at long wavelengths.

Science goals motivate the broadest tuning range and bandwidth possible. These goals include enhancing the contrast between both intrinsic and extrinsic emission and propagation processes; the study of SNRs [12]; the study of the interstellar medium (ISM) of the Milky Way and external galaxies [20]; the study of self-absorption processes in extragalactic sources [14]; the study of pulsars; and the study of ionospheric turbulence and waves [21]. However, the increasing opacity of the ionosphere at low frequencies combined with overwhelming interference from commercial broadcast FM radio stations pose a practical limit of ~ 3 to ~ 88 MHz. Accounting for the $\sim 4 : 1$ bandwidth that can be achieved by active antennas (Section III-A), we expect to meet most of our requirements in the frequency range 20–80 MHz, and to be able to do useful science, albeit with reduced capability, in 10–20 and 80–88 MHz.

As discussed in Section III-D, LWA station digital electronics will have the ability to form multiple beams, each of which can be pointed and tuned independently of the others, with only a modest increase in the cost and complexity relative to what is required to form a single beam. We have settled on a specification of three beams for most stations. One of these beams will always be available to assist in measuring the ionosphere, as part of image calibration [22], whereas the other two can be used for simultaneous independent observing programs. Due to practical limitations in data transmission from stations to the correlator (Section IV), we constrain the bandwidth

for multibeam operation to 8 MHz (selectable from anywhere with the tuning range). However, beams will be formed at the station as “full RF;” i.e., with bandwidth equal to the tuning range. LWA “core” stations—i.e., ~ 15 stations located within the central 10 km of the LWA—will be equipped to send one additional beam consisting of the full RF bandwidth to the correlator simultaneously with the three 8 MHz beams. This beam will be used primarily for solar science during the day and primarily for early universe (“Dark Ages”) studies at night.

The specifications arising from requirements for long-wavelength astrophysics lead to an instrument that is also well suited to study of the ionosphere. This is because astrophysical image calibration requires solving for the refractive effects of the ionosphere, thereby resulting in precise measurements of fine structure over the array as side information. Variations in total electron content (ΔTEC) produce phase variations $\sim 0.85(\Delta\text{TEC}/10^{13} \text{ cm}^{-2}) (100 \text{ MHz}/\nu)$. ΔTEC measurements at levels below 10^{12} cm^{-2} have already been demonstrated using the VLA (using just 1.6 MHz bandwidth at 74 MHz), and one can obtain complementary measurements that enhance the value of space-based and other ionospheric remote sensing measurements; e.g., [23]. The increased bandwidth and sensitivity of LWA may enable measurements necessary to improve existing regional and global assimilating models [24], [25] used to understand and predict ionospheric behavior.

III. STATION-LEVEL DESIGN

A. Active Antennas

To achieve large tuning range, previous broadband low-frequency telescopes such as the Clark Lake TPT [26] and UTR-2 [27] used antennas that have inherently large impedance bandwidth—conical spirals and “fat” dipoles, respectively. Such antennas are mechanically complex, making them expensive, difficult to construct, and prone to maintenance problems. This makes them unsuitable as elements in arrays on the scale of LWA. In contrast, simple wire dipoles are mechanically very well suited for use in large low-frequency arrays but have inherently narrow impedance bandwidth. However, this is not necessarily a limitation below ~ 300 MHz because the natural Galactic noise which is transmitted through an impedance mismatch can potentially dominate over the noise contribution of the front-end electronics [28], [29]. For this reason, we consider the antenna and first stage of gain as a single component, which we refer to as an “active antenna.”

The minimum acceptable ratio of Galactic to internal noise from an active antenna is determined by integration time: The smaller the ratio, the greater the integration time required to achieve a specified sensitivity. For example, integration time is increased by 57% and 21% over the ideal (zero internal noise) values for domination ratios of

6 and 10 dB, respectively [30]. Once the antenna system is “minimally” galactic noise-limited, further improvement in impedance match has little effect on the sensitivity of the instrument. Since Galactic noise is broadband and distributed over the entire sky, further improvement in the sensitivity of the telescope can therefore be achieved only by adding antennas.

The noise temperature at the output of an active antenna is given by $T_{\text{sys}} = \xi T_A + T_p$, where T_A is the antenna temperature, T_p is the noise temperature of the electronics, and ξ is impedance mismatch efficiency; that is, the fraction of power captured by the antenna that is successfully transmitted to the electronics. This is given by $(1 - |\Gamma|^2)$, where Γ is the reflection coefficient at the antenna terminals. If T_A is dominated by the Galactic noise, then $T_A \approx T_{74}(\lambda/4 \text{ m})^{2.6}$, where T_{74} is approximately 2000 K and λ is wavelength [28]. Although the ground is normally radiometrically “cold” relative to the sky at these frequencies, a conducting ground screen is important to prevent loss through absorption into the ground [29] and also to stabilize the system temperature by isolating the antenna from variable (e.g., dry versus wet) ground conditions [31].

Candidate antenna structures for LWA stations are shown in Fig. 3. The “big blade” [32] exhibits the best overall performance, whereas the “fork” antenna [33] performs slightly less well but seems to be better suited to manufacture in large quantities. For purposes of subsequence analysis in this paper, we shall assume the big blade; however, the differences from the fork and other design concepts are minor [32], [34].

The LWA candidate front-end electronics (located at the antenna feedpoint) employs commercial InGaP heterostructure bipolar transistor monolithic microwave integrated circuit amplifiers (Mini-Circuits GALI-74) in a differential configuration presenting a 100 Ω balanced load to the antenna. This is followed by a passive balun which produces a 50 Ω single-ended signal suitable for transmission over coaxial cable. The total gain, noise temperature, and input 1 dB compression point are approximately 36 dB, 250 K, and -18 dBm, respectively, and approximately independent of frequency over 10–88 MHz.

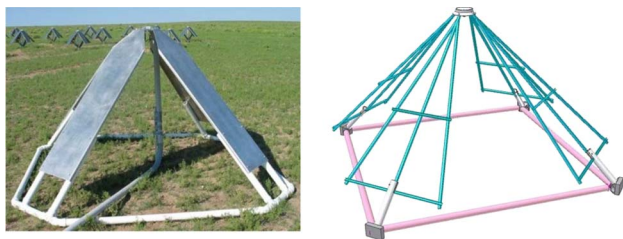


Fig. 3. LWA candidate antennas. (a) “Big blade” design and (b) “fork” design. Antennas are approximately 1.5 m high. Arms are tilted downward to primarily improve pattern.

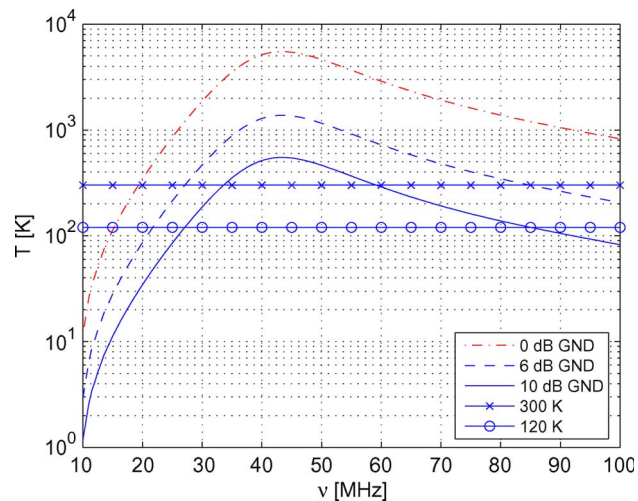


Fig. 4. Maximum T_p that yields the indicated degree of Galactic noise domination (GND) into 100 Ω for the LWA candidate antenna.

Alternative designs providing significantly lower noise temperature are possible; however, the compression point of such designs is correspondingly lower, which increases the risk of being driven into compression by RFI.

The condition for Galactic noise-limited sensitivity is

$$T_p \ll \xi T_{74} \left(\frac{\lambda}{4 \text{ m}} \right)^{2.6}. \quad (1)$$

Fig. 4 demonstrates that T_p primarily determines the bandwidth, and only secondarily the sensitivity, of an active antenna. For example, the LWA candidate front end (assuming 300 K to be conservative) yields output in which Galactic noise dominates over internal noise by at least 6 dB from 27 to 85 MHz. This is verified experimentally in Section III-D (Fig. 6).

The collecting area of a single antenna in isolation A_{e0} is a function of λ , zenith angle θ , and azimuth ϕ . Dependence of the gain on θ and ϕ can be modeled as a factor of $\cos^{\alpha(\phi)} \theta$. Examination of the big blade patterns from [32] suggests $\alpha = 1.34$ in the E-plane and $\alpha = 1.88$ in the H-plane. For simplicity, we assume a single value of $\alpha = 1.6$ (the geometric mean of 1.34 and 1.88). Effective collecting area can then be expressed as

$$\xi A_{e0}(\lambda, \theta) = \xi G(\lambda) \frac{\lambda^2}{4\pi} \cos^{1.6} \theta. \quad (2)$$

For the big blade, the zenith directivity $G(\lambda)$ ranges from about 8.5 dB at 20 MHz to 5.9 dB at 88 MHz, assuming an electrically large ground screen [32]. This model is known to be quite good below 65 MHz. At higher frequencies, the

pattern becomes complex; by 74 MHz, a small deviation from the simple cosine power law is apparent, and by 88 MHz, the E-plane pattern has bifurcated. Nevertheless, the model is useful in the next section, in which we aim to determine the number of active antennas required per station.

B. Collecting Area Requirement

The primary parameters in the design of the station array are collecting area, which contributes to image sensitivity; and the dimensions of the station beam, which constrains the image FOV. The primary constraint in determining the required collecting area is being able to detect a sufficient number of sources $N_{\text{FOV}}(s)$ above a certain flux s within the FOV to calibrate the image against the distorting effects of the ionosphere. At 74 MHz, the number of sources per square degree with flux density s or greater is

$$N(s) \approx 1.14 \left(\frac{s}{\text{Jy}} \right)^{-1.3} \quad (3)$$

with the caveat that this is only known to be accurate down to about $s = 0.4$ Jy. To extrapolate to other frequencies, it is assumed that s scales according to the typical spectral index of a low-frequency source; i.e., as $\lambda^{+0.7}$. Thus we have

$$N(s) = 1.14 \left(\frac{s}{\text{Jy}} \right)^{-1.3} \left(\frac{\lambda}{4 \text{ m}} \right)^{0.91}. \quad (4)$$

The FOV of the LWA can be defined as the angular area bounded by the half-power beamwidth of a station beam. In the elevation plane, this is given by $\psi(\theta) \approx \psi_0(\lambda/D) \sec \theta$ rad, where D is the station mean diameter and $\psi_0 = 1.02$ for a uniformly excited circular array. In the orthogonal plane, the beamwidth is simply $\psi_0(\lambda/D)$. FOV can then be expressed as

$$\text{FOV} = 4.12 \psi_0^2 \left(\frac{\lambda}{4 \text{ m}} \right)^2 \left(\frac{D}{100 \text{ m}} \right)^{-2} \sec \theta [\text{deg}^2]. \quad (5)$$

The number of sources with flux density $\geq s$ in the FOV is therefore given by the product of (4) and (5).

The required number of sources is uncertain. Ideally, we use at least one calibrator per isoplanatic patch. However, because imaging has never been attempted at these frequencies and baseline lengths, the appropriate patch size is unknown. The best we can do at present is to compare to the number of calibrators needed for imaging with the 74 MHz VLA using field-based calibration [35]. Extrapolating these results to the LWA provides a basis for making rough estimates. In its largest configuration, the VLA requires four to six sources typically, with ten sources

desirable. Let this number be $N_{\text{cal}}^{\text{VLA}}$. The requirement for LWA can be extrapolated as follows:

$$N_{\text{cal}} = N_{\text{cal}}^{\text{VLA}} \left(\frac{L_B}{36 \text{ km}} \right)^2 \left(\frac{\text{FOV}}{\text{FOV}_{\text{VLA}}} \right) \frac{1}{r_{\text{np}}} \left(\frac{\lambda}{4 \text{ m}} \right)^2 \quad (6)$$

where L_B is the length of maximum baseline included on the assumption that N_{cal} grows in proportion to the number of resolution elements in the FOV; $\text{FOV}_{\text{VLA}} = 77 \text{ deg}^2$ is the FOV of the VLA at 74 MHz; and r_{np} is the fraction of detectable sources that are usable point sources (e.g., not apparently extended due to the improved resolution). In this expression, the wavelength dependence accounts for the fact that the number of calibrators required scales by another factor of λ^2 because the magnitude of ionospheric phase variations is proportional to λ .

To determine if N_{cal} sources are detectable in the FOV, it is necessary to develop an expression for imaging sensitivity. The root mean square image noise level σ is given by [9]

$$\sigma = \frac{2kT_{\text{sys}}}{\eta_s A_{\text{es}} \sqrt{N_S(N_S - 1)N_{\text{pol}}\Delta\tau\Delta\nu}} \quad [\text{Wm}^{-2}\text{Hz}^{-1}] \quad (7)$$

where $k = 1.38 \times 10^{-23}$ J/K, A_{es} is the collecting area of a station, N_S is the number of stations, $N_{\text{pol}} = 2$ is the number of orthogonal polarizations, $\Delta\tau$ is the total observation time, $\Delta\nu$ is the observed bandwidth, and η_s accounts for the aggregate effect of various hard-to-characterize losses throughout the system.

The effective collecting area of a station is given by

$$A_{\text{es}} = \gamma N_a \xi A_{e0}(\lambda, \theta, \phi) \quad (8)$$

where N_a is the number of dual-polarization antennas in the station and γ is a coefficient that accounts for the aggregate effect of mutual coupling. It is known from modeling experiments that γ is in the range 1 ± 0.35 (variation with respect to θ and ϕ) for a station consisting of straight dipoles near resonance at 38 MHz [36]. This may or may not also be the case for a station consisting of LWA candidate antennas at this or other frequencies, but it seems unlikely to be dramatically different. Making the substitutions, we find

$$N_a \geq (1.75 \times 10^5) r_C \left[\left(\frac{\lambda}{4 \text{ m}} \right)^{3.44} + \frac{T_p}{\xi T_{74}} \left(\frac{\lambda}{4 \text{ m}} \right)^{0.84} \right] \times \left(\frac{A_{e0}(\lambda, \theta, \phi)}{\text{m}^2} \right)^{-1} \left(\frac{N_{\text{cal}}^{\text{VLA}}}{r_{\text{np}}} \right)^{0.77} \left(\frac{L_B}{36 \text{ km}} \right)^{1.54} \quad (9)$$

where

$$C = \left[\eta_s \gamma \sqrt{N_s(N_s - 1)N_{\text{pol}}\Delta\tau\Delta\nu} \right]^{-1} \quad (10)$$

and r is the required signal-to-noise ratio for detecting the calibrators. It is interesting to note that this result does not depend on the station size D since the number of available calibrators scales in proportion to the beamwidth.

The results are shown in Fig. 5. These results assume the big blade antenna of [32] (but should be approximately the same for other candidate antenna designs), $r = 5$, $\eta_s = 0.78$, $\Delta\tau = 6$ s, and $\Delta\nu = 8$ MHz. The value of $\Delta\tau$ is chosen to be the maximum time interval over which the ionospheric phases will not vary significantly. This is ~ 6 s based on 1) the assumption that phase variations are proportional to wavelength and 2) our experience that a 1 min solution interval was sufficient for the VLA, which is roughly one-tenth the size of LWA. The results are shown for three values of T_p to demonstrate the weak influence of receiver noise temperature. It is clear that much depends on the beam pointing elevation, with N_a increasing with increasing zenith angle. This is due primarily to the antenna pattern. On the other hand, note that N_a is dramatically reduced if we assume alternative (reasonable, but less conservative) calibratability assumptions. Taken together, from an image calibratability viewpoint, arguments can be made for N_a as small as 50 and as large as 2500.

Additional considerations in the N_a decision are system cost, which scales roughly linearly with N_a and motivates minimizing N_a ; and image thermal noise sensitivity σ , given by (7). Choosing $N_a = 256$ (arbitrarily chosen to be a

power of two) yields $\sigma \sim 1$ mJy over 20–80 MHz for $\Delta\tau = 1$ h (all other parameters the same). This meets the sensitivity goals pertaining to science requirements while achieving a balance with classical and sidelobe confusion (see Section II) for 400 km baselines over plausible integration times. From Fig. 5, this also seems to facilitate image calibration over a broad range of frequencies and zenith angles. Although this analysis suggests $N_a = 256$ will be challenging for calibration at lower elevations, increasing N_a is costly. Moreover, present estimates do not consider emerging calibration techniques; e.g., leveraging the known frequency dependence of ionospheric phase fluctuations across a wide bandwidth. Finally, previous dipole-array based observations from a comparable latitude to as far south as the Galactic center ($\delta \approx -29^\circ$ declination, corresponding to a maximum elevation of $\approx 27^\circ$ above the southern horizon [37]) and beyond ($\delta < -40^\circ$ [38]) have produced important science despite these limitations.

C. Array Geometry

Given that the station should have a diameter of about 100 m and $N_a = 256$, the mean spacing between antennas will be 5.4 m, which is 0.36λ and 1.44λ at 20 and 80 MHz, respectively. Traditional techniques for broadband array design require uniform spacings less than 0.5λ at the highest frequency of operation [39]. This is for two reasons: 1) to prevent spatial aliasing and 2) to use the strong electromagnetic coupling to stabilize the scan impedance of the individual antennas, improving bandwidth. However, to achieve this spacing at 80 MHz requires an increase in N_a by more than a factor of three, which is cost-prohibitive. Implementing larger N_a using a hierarchical (i.e., subarray-based) architecture allows

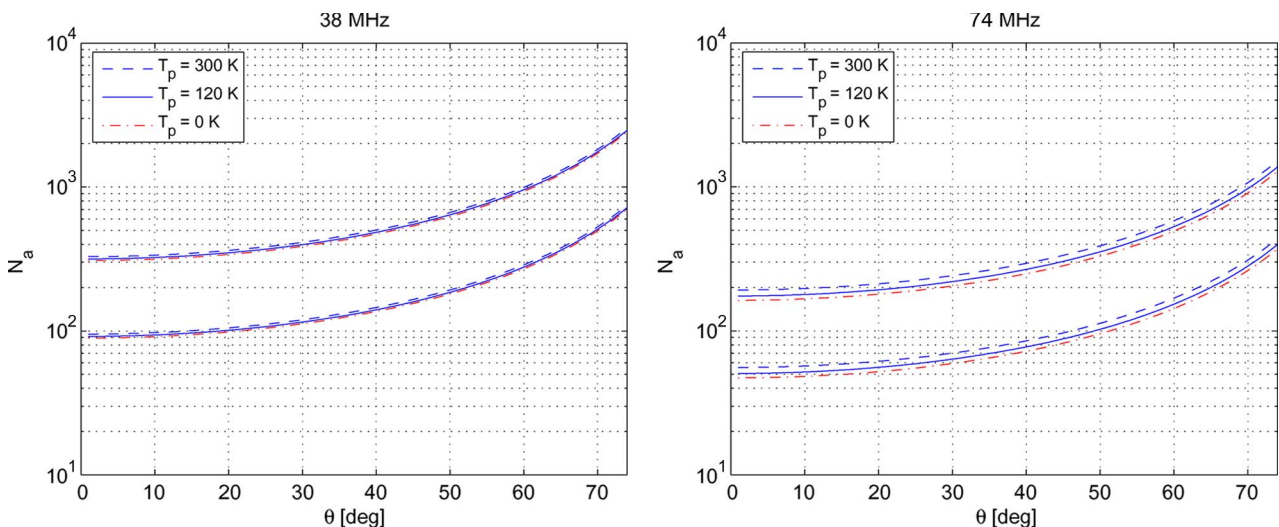


Fig. 5. Required number of dual-polarization antennas per station (N_a) for $N_s = 53$ with $L_B = 400$ km. (a) 38 and (b) 74 MHz. The upper set of curves assume $N_{\text{cal}}^{\text{VLA}} = 10$ and $r_{\text{np}} = 0.5$, whereas the lower set of curves assume $N_{\text{cal}}^{\text{VLA}} = 4$ and $r_{\text{np}} = 1$. The right edge of each plot corresponds to upper culmination of the Galactic Center as seen from New Mexico.

more antennas at similar cost, but only by sacrificing the ability for beams to be steered independently over the entire sky. For these reasons, we have chosen to address the spatial aliasing problem by arranging the antennas in pseudorandom fashion. Although the specific geometry has not yet been selected, the current plan is to enforce a minimum spacing constraint of 5 m.

Various ionospheric, solar, and especially Galactic science goals require the ability to observe towards declinations that appear low in the southern sky from New Mexico. To compensate for the elevation-plane widening of the beam for these observations, the station footprint will be an ellipse with NS:EW axial ratio $\sim 1.2 : 1$. This results in a circular station beam at transit for the celestial equator.

D. Station Electronics

In our preliminary design, the signal from every antenna is processed by a dedicated direct-sampling receiver consisting of an analog receiver (ARX) and an analog-to-digital converter (A/D), which samples 196 million samples per second (MSPS). Beams are formed using a time-domain delay-and-sum architecture, which allows the entire 10–88 MHz passband associated with each antenna to be processed as single wide-band data stream. Delays are implemented in two stages: A coarse delay is implemented using a first-in first-out buffer operating on the A/D output samples, followed by a finite impulse response filter. The signals are then added to the signals from other antennas processed similarly. Three or four dual-polarization beams of bandwidth 78 MHz, each capable of fully independent pointing over the visible sky, will be constructed in this fashion.

These beams will be available for various “backends” implemented at the station level, such as data recorders, wide-band spectrometers, and pulsar machines. For interferometric imaging, two “tunings” will be extracted from any frequency in the 78-MHz-wide passband, having bandwidth selectable between 400 kHz and 8 MHz divided into 4096 spectral channels. This is the output to the LWA correlator. As explained in Section II, stations in the LWA core will also output a wide-band beam derived from one of the full-RF beams.

To facilitate commissioning activities, diagnostics, and certain types of science observations requiring all-sky FOV, the station electronics will also have the capability to coherently capture and record the output of all A/Ds, where each A/D corresponds to one antenna. This will occur in two modes: the “transient buffer—wide-band” (TBW) allows the raw output of the A/Ds to be collected continuously but only for ~ 100 ms at a time. The “transient buffer—narrow-band” (TBN), in contrast, allows a single tuning of ~ 100 kHz bandwidth to be recorded indefinitely.

Considerations in the design of direct sampling receivers for low-frequency radio astronomy are summarized in [40]. In a direct sampling receiver, the analog signal path involves only gain and filtering, and the sky signal is sampled without frequency conversion. The primary

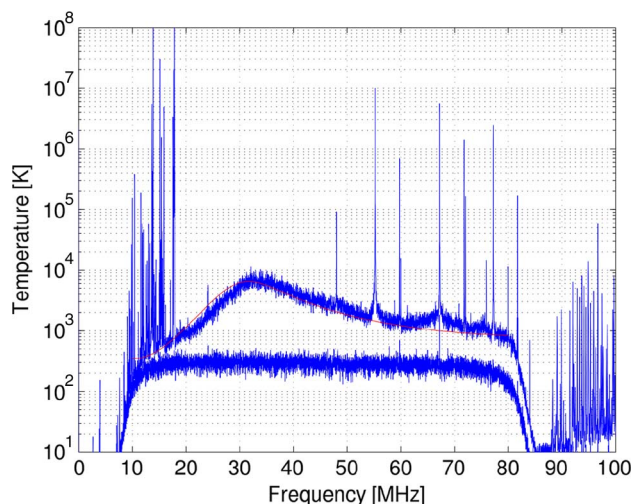


Fig. 6. (Top curve) Spectrum acquired using an LWA prototype active antenna (similar to that shown in the right of Fig. 3), with the ARX and A/D described in the text; 1 s integration. Also shown overlaying the top curve is the result predicted from a sky model. (Bottom curve) Same measurement performed with a $100\ \Omega$ (matched) load replacing the dipole arms.

considerations in choosing a direct-sampling architecture, as opposed to a more traditional tuning superheterodyne architecture, are simplicity (e.g., no local oscillators, no mixers, etc.) and simultaneous access to the entire 10–88 MHz tuning range. The primary difficulty is applying sufficient gain to maintain Galactic noise dominance over receiver and quantization noise, with sufficient linearity and headroom to accommodate RFI.

The latter task is complicated by the varying nature of RFI over the tuning range. RFI impacts astronomy at two levels: first, by creating a potential threat to linearity; and secondly, by obstructing spectrum of interest. We consider the linearity issue first. At the remote rural locations at which stations are to be located, the most troublesome interference is due to distant transmitters at frequencies below about 30 MHz, whose signals arrive at the station by refraction from the ionosphere. Television signals in 54–88 MHz and FM broadcast signals in 88–108 MHz rank second at most rural sites in terms of overall RFI power delivered to the antennas, but this has potential to become more serious for stations located closer to population centers.⁴ RFI in the spectrum between 30 and 54 MHz is primarily local two-way radio and is normally only an intermittent problem from a linearity perspective.

To accommodate the various uncertainties in the RFI environment, we have developed an ARX that can be

⁴The effect of the transition from analog to digital TV in the United States, currently planned to be complete by February 2009, is uncertain. Although the spectral characteristics of digital TV signals are more troublesome from an astronomy viewpoint, it appears that fewer broadcasters will be operating in the region after the transition. Also, the digital transition mandate does not apply to certain classes of analog low-power and repeater stations.

electronically reconfigured between three modes: a full-bandwidth (10–88 MHz) uniform-gain mode, a full-bandwidth dual-gain mode in which frequencies below about 40 MHz can be attenuated using a “shelf filter,” and a 28–54 MHz mode, which serves as a last line of defense in the case where RFI above and/or below this range is persistently linearity-limiting. In addition, the total gain in each mode can be adjusted over a 60 dB range in 2 dB steps, allowing fine adjustments to optimize the sensitivity–linearity tradeoff.

This choice of modes and gain settings was based on a detailed study of RFI at the VLA, combined with a study of A/D capabilities, leading to the conclusion that an A/D of about 200 MSPS with 8-bit sampling was probably sufficient when combined with an ARX having the capabilities described above [41]. We currently favor a sampling rate $F_s = 196$ MSPS, as this results in the highly desirable situation that the 88–108 MHz FM broadcast band aliases onto itself, which greatly reduces antialias filtering requirements.

A prototype digitizer using the Analog Devices AD9230-250 12-bit A/D has been constructed and tested in conjunction with a prototype ARX having the characteristics described above, in field conditions. (The use of 12-bit sampling over 8-bit sampling provides some additional headroom without much impact on cost or power.) The results have been excellent and are shown in Fig. 6. Note that the result is sky-noise dominated by at least 6 dB over the range 20–80 MHz, and by at least 10 dB in 28–47 MHz. Also note that this is achieved despite the presence of very strong in-band RFI. The system input 1 dB compression point, as configured for this measurement, was -45 dBm.

Experience from the 74 MHz VLA system and other instruments has demonstrated that RFI from external as well as internal sources will be present at all levels throughout the spectrum. The primary difficulty posed by RFI, assuming it is not linearity-threatening, is that it dramatically increases the amount of manual effort required to reduce data [7]. A variety of countermeasures to facilitate automatic real-time mitigation of RFI are known [42] and being considered for implementation. In the station electronics, this may include the ability to modify the response of digital filters to suppress narrow-band RFI and pulse blanking to remove strong, bursty interference. Spatial or space-frequency nulling can potentially be supported by the planned electronics architecture. For spectrometry, time-frequency blanking to resolutions of a few milliseconds \times a few kilohertz is supported. Other devices and backends may use additional application-specific methods, and the specific mix of techniques employed will depend on the observing mode and RFI present.

IV. INTERFEROMETER-LEVEL DESIGN

LWA stations will be connected by gigabit ethernet over optical fiber to a centrally located correlator. For most stations, the output to the correlator will be both

polarizations of three beams of 8 MHz bandwidth each, resampled to 8 bits at 1.5 times the Nyquist rate. This results in a data rate of 576 Mb/s. LWA core stations will also transmit a wide-band beam (Section II), which increases the data rate for these stations to 1920 Mb/s.

The purpose of the correlator is to compute the correlations between stations, which, by application of the Van Cittert–Zernicke theorem, can then be transformed into a raw image within the beam FOV [9] and subsequently calibrated (typically as a postprocessing step) to obtain the desired image. The large number of high-data-rate signals involved make correlation extremely computationally intensive, requiring dedicated equipment running in real time for the complete LWA. Development of this correlator has not yet begun. However, as discussed in Section V, the LWA is to be built in stages, with the number of stations available in the early stages being relatively small. During this time, we intend to simply capture the station outputs using disk buffers and perform correlation in software using general-purpose computers.

A demanding aspect of image calibration is correction for the dynamically-varying refractive effects of the ionosphere. As mentioned in Section II, our intent is to measure ionospheric corrections over the entire sky in real time from each station using a “calibration beam” in addition to the two imaging beams. This beam will cycle rapidly (< 10 s) among ~ 100 bright sources, sampling differences in total electron content over more than 5000 different lines-of-sight through the ionosphere [22].

V. CONCLUDING REMARKS

LWA has much in common with LOFAR (mentioned in Section I), in particular its low-band (30–80 MHz) subsystem. However, there are significant differences that make them complementary instruments. LWA will be able to observe to much lower frequencies: as low as 10 MHz. LOFAR is located in Northern Europe (latitude $\approx 55^\circ$ N), favoring extragalactic sources, whereas LWA will be located at $\approx 34^\circ$ N, offering access to the important inner Galaxy region. LWA’s larger and more densely packed stations ($N_a = 256$ for LWA as opposed to 48 or 96 for LOFAR) are more suited to targeted observations (again, well suited for galactic work), whereas the LOFAR design favors extragalactic surveys.

The LWA project conducted a system requirements review in Fall 2007 and is currently (October 2008) preparing to conduct a preliminary design review for LWA-1, the first LWA station. The cost of each LWA station is currently estimated at \$850 000. Based on current funding projections, LWA Stations 1–3 will be constructed by the end of 2010, Stations 4–10 in 2011, and Stations 11–16 in 2012. A schedule for Stations 17–53 has not yet been determined and will depend on future funding.

Useful science observations will be possible at each stage of development. Each station by itself will be a capable

radio telescope comparable to or exceeding the collecting area of most past and present low-frequency instruments. Single-station science goals include observation of radio recombination lines from the cold ISM with improved sensitivity, frequency coverage, and angular resolution [43]; sensitive broadband observations of ~ 80 pulsars [44]; and searches for galactic and extragalactic radio transients [45], [46]. With $N_S \sim 9$, imaging with resolution $< 10''$ will be possible for hundreds of sources ≥ 10 Jy [47], including many radio galaxies. Expansion to $N_S = 16$ stations will add short baselines and bring improved surface brightness sensitivity for targets including SNRs and clusters of galaxies [48]. The threshold for full-field calibration and

mapping is unknown but will probably require completion of at least half the total complement of 53 stations. ■

Acknowledgment

The authors thank B. Erickson, whose early development of prototype antennas and broader experience across many scientific, technical, and practical aspects of low-frequency radio astronomy remain an invaluable guide. In addition to the efforts of the many members of the many institutions involved in LWA, they acknowledge the specific contributions of M. Harun, B. Hicks, N. Paravastu, and P. Ray to the work described in this paper.

REFERENCES

- [1] P. F. Goldsmith, Ed., *Instrumentation and Techniques for Radio Astronomy*. New York: IEEE Press, 1988.
- [2] N. E. Kassim and K. W. Weiler, *Low Frequency Astrophysics From Space*. Berlin, Germany: Springer-Verlag, 1990, ser. Lecture Notes in Physics, vol. 362.
- [3] R. G. Stone, K. W. Weiler, M. L. Goldstein, and J.-L. Bougeret, Eds., *Radio Astronomy at Long Wavelengths*. Washington, DC: American Geophysical Union, 2000, Geophysical Monograph 119.
- [4] N. E. Kassim, M. R. Perez, W. Junor, and P. A. Henning, Eds., *Clark Lake to the Long Wavelength Array: Bill Erickson's Radio Science*, ASP Conf. Ser., vol. 345, 2005.
- [5] T. J. Pearson and A. C. S. Readhead, "Image formation by self-calibration in radio astronomy," *Annu. Rev. Astron. Astrophys.*, vol. 22, pp. 97–130, 1984.
- [6] N. E. Kassim, R. A. Perley, W. C. Erickson, and K. S. Dwarakanath, "Subarcminute resolution imaging of radio sources at 74 MHz with the very large array," *Astron. J.*, vol. 106, pp. 2218–2228, 1993.
- [7] N. E. Kassim et al., "The 74 MHz system on the very large array," *Astrophys. J. Suppl. Ser.*, vol. 172, pp. 686–719, Oct. 2007.
- [8] N. E. Kassim et al., "The long wavelength array," in *Clark Lake to the Long Wavelength Array: Bill Erickson's Radio Science*, ASP Conf. Ser., vol. 345, 2005, pp. 392–398.
- [9] A. R. Thompson, J. Moran, and G. Swenson, Jr., *Interferometry and Synthesis in Radio Astronomy*, 2nd ed. New York: Wiley, 2001.
- [10] H. R. Butcher, "LOFAR: First of a new generation of radio telescopes," in *Proc. SPIE*, Sep. 2004, vol. 5489, pp. 537–544.
- [11] T. E. Clarke, "Scientific requirements for the long wavelength array," Memo 117 ver. 2.3, Nov. 19, 2007, Long Wavelength Array Memo Series. [Online]. Available: <http://www.phys.unm.edu/~lwa/memos>
- [12] C. L. Brogan, "Resolving the confusion: Recent low frequency observations of the galaxy," in *Clark Lake to the Long Wavelength Array: Bill Erickson's Radio Science*, ASP Conf. Ser., vol. 345, 2005, pp. 187–196.
- [13] D. E. Harris, "From Clark Lake to Chandra: Closing in on the low end of the relativistic electron spectra in extragalactic sources," in *Clark Lake to the Long Wavelength Array: Bill Erickson's Radio Science*, ASP Conf. Ser., vol. 345, 2005, pp. 254–263.
- [14] T. J. W. Lazio et al., "Cygnus A: A long-wavelength resolution of the hot spots," *Astrophys. J.*, vol. 642, pp. 33–36, 2006.
- [15] A. Cohen, "Estimates of the classical confusion limit for the LWA," Memo 17, Dec. 2004, Long Wavelength Array Memo Series. [Online]. Available: <http://www.phys.unm.edu/~lwa/memos>
- [16] T. J. W. Lazio et al., "The radiometric noise law and extrasolar planets," *Astrophys. J.*, vol. 612, pp. 511–518, 2004.
- [17] I. de Pater, "Low frequency planetary radio emissions," in *Clark Lake to the Long Wavelength Array: Bill Erickson's Radio Science*, ASP Conf. Ser., vol. 345, 2005, pp. 154–166.
- [18] M. J. Jarvis et al., "Near-infrared K-band imaging of a sample of ultra-steep-spectrum radio sources selected at 74 MHz," *Mon. Not. Royal Astron. Soc.*, vol. 355, pp. 20–30, 2004.
- [19] J. J. Condon, "Extragalactic astronomy at low frequencies," in *Clark Lake to the Long Wavelength Array: Bill Erickson's Radio Science*, ASP Conf. Ser., vol. 345, 2005, pp. 237–253.
- [20] T. J. W. Lazio, "Galactic astronomy at long wavelengths: Past prologue," in *Clark Lake to the Long Wavelength Array: Bill Erickson's Radio Science*, ASP Conf. Ser., vol. 345, 2005, pp. 217–224.
- [21] A. R. Jacobson and W. C. Erickson, "Observations of electron density irregularities in the plasmasphere using the VLA radio interferometer," *Ann. Geophys.*, vol. 11, no. 10, pp. 869–888, Oct. 1993.
- [22] A. Cohen and N. Paravastu, "Probing the ionosphere with the LWA by rapid cycling of celestial radio emitters," Memo 128, Mar. 2008, Long Wavelength Array Memo Series. [Online]. Available: <http://www.phys.unm.edu/~lwa/memos>
- [23] K. F. Dymond et al., "The combined radio interferometry and COSMIC experiment in tomography (CRICKET) campaign," in *Proc. 2008 Ionospheric Effects Symp.*, Alexandria, VA, May 13–15, 2008.
- [24] R. W. Schunk, L. Scherliess, J. J. Soyka et al., "Global assimilation of ionospheric measurements (GAIM)," *Radio Sci.*, vol. 39, RS1502, 2004, doi: 10.1029/2002RS002794.
- [25] G. S. Bust, T. W. Garner, and T. L. Gaussion, "Ionospheric data assimilation three-dimensional (IDA3D): A global, multisensor, electron density specification algorithm," *J. Geophys. Res.*, vol. 109, A11312, 2004.
- [26] W. C. Erickson, M. J. Mahoney, and K. Erb, "The Clark Lake teepee-tee telescope," *Astrophys. J. Suppl. Ser.*, vol. 50, no. 403, pp. 403–420, Nov. 1982.
- [27] S. Y. Braude et al., "Decametric survey of discrete sources in the northern sky: I. The UTR-2 radio telescope. Experimental techniques and data processing," *Astrophys. Space Sci.*, vol. 54, pp. 3–36, 1978.
- [28] S. W. Ellingson, "Antennas for the next generation of low frequency radio telescopes," *IEEE Trans. Antennas Propag.*, vol. 53, pp. 2480–2489, Aug. 2005.
- [29] S. W. Ellingson, J. H. Simonetti, and C. D. Patterson, "Design and evaluation of an active antenna for a 29–47 MHz radio telescope array," *IEEE Trans. Antennas Propag.*, vol. 55, pp. 826–831, Mar. 2007.
- [30] W. C. Erickson, "Integration times vs. sky noise dominance," Memo 23, Aug. 2005, Long Wavelength Array Memo Series. [Online]. Available: <http://www.phys.unm.edu/~lwa/memos>
- [31] N. Paravastu, B. Hicks, E. Aguilera et al., "Impedance measurements of the big blade and fork antennas on ground screens at the LWDA site," Memo 90, Jun. 2007, Long Wavelength Array Memo Series. [Online]. Available: <http://www.phys.unm.edu/~lwa/memos>
- [32] S. W. Ellingson and A. Kerkhoff, "Comparison of two candidate elements for a 30–90 MHz radio telescope array," in *Proc. Int. Symp. Antennas Propag.*, Washington, DC, Jul. 2005, vol. 1A, pp. 590–593.
- [33] N. Paravastu, B. Hicks, P. Ray, and W. Erickson, "A candidate active antenna design for a low frequency radio telescope array," in *Proc. Int. Symp. Antennas Propag.*, Honolulu, HI, Jun. 2007, pp. 4493–4496.
- [34] A. Kerkhoff and H. Ling, "Application of pareto genetic algorithm optimization to the design of broadband dipole elements for use in the Long Wavelength Array (LWA)," in *Proc. Int. Symp. Antennas Propag.*, Honolulu, HI, Jun. 2007, pp. 2201–2204.
- [35] A. S. Cohen et al., "The VLA low-frequency sky survey," *Astron. J.*, vol. 134, no. 3, pp. 1245–1262, Sep. 2007.
- [36] S. W. Ellingson, "Effective aperture of a large pseudorandom low-frequency dipole array," in *Proc. Int. Symp. Antennas Propag.*, Honolulu, HI, Jun. 9–15, 2007, pp. 1501–1504.
- [37] N. E. Kassim, T. N. LaRosa, and W. C. Erickson, "Steep spectrum radio lobes near the galactic centre," *Nature*, vol. 322, pp. 522–524, 1986.
- [38] W. C. Erickson and M. J. Mahoney, "Clark Lake observations of IC 443 and Puppis A," *Astrophys. J.*, vol. 290, pp. 596–601, 1985.
- [39] R. C. Hansen, *Phased Array Antennas*. New York: Wiley, 1998.
- [40] S. W. Ellingson, "Receivers for low-frequency radio astronomy," in *Clark Lake to the Long Wavelength Array: Bill Erickson's Radio Science*, ASP Conf. Ser., vol. 345, 2005.

- [41] S. Ellingson, "LWA analog signal path planning," Memo 121 ver. 2, Feb. 2008, Long Wavelength Array Memo Series. [Online]. Available: <http://www.phys.unm.edu/~lwa/memos>
- [42] ITU, "Techniques for mitigation of radio frequency interference in radio astronomy," ITU-R Rep. RA.2126, 2007.
- [43] W. C. Erickson, D. McConnell, and K. R. Anantharamaiah, "Low frequency carbon recombination lines in the central regions of the galaxy," *Astrophys. J.*, vol. 454, pp. 125–133, 1995.
- [44] B. A. Jacoby, W. M. Lane, and T. J. W. Lazio, "Simulated LWA-1 pulsar observations," Memo 104, Sep. 2007, Long Wavelength Array Memo Series. [Online]. Available: <http://www.phys.unm.edu/~lwa/memos>
- [45] S. D. Hyman, T. J. W. Lazio, N. E. Kassim, P. S. Ray, C. B. Markwardt, and F. Yusef-Zadeh, "A powerful bursting radio source towards the Galactic Centre," *Nature*, vol. 434, pp. 50–52, 2005.
- [46] G. C. Bower, "Mining for the ephemeral," *Science*, vol. 318, no. 5851, pp. 759–760.
- [47] A. Cohen, T. Clarke, and J. Lazio, "Early science from the LWA phase II: A target list," Memo 80, Feb. 12, 2007, Long Wavelength Array Memo Series. [Online]. Available: <http://www.phys.unm.edu/~lwa/memos>
- [48] T. E. Clarke, "The long and short of it: Clusters of galaxies at low frequencies and high energies," in *Clark Lake to the Long Wavelength Array: Bill Erickson's Radio Science*, ASP Conf. Ser., vol. 345, 2005, pp. 227–236.